The role of endothelial autocrine NRG1/ERBB4 signaling in cardiac remodeling

Reference:
Dugaucquier Lindsey, Feyen Eline, Mateiu Ligia, Bruyns Tine Anne Marie, De Keulenaer Gilles, Segers Vincent F.M..- The role of endothelial autocrine NRG1/ERBB4 signaling in cardiac remodeling
American journal of physiology : heart and circulatory physiology / American Physiological Society- ISSN 0363-6135 - 319:2(2020), p. H443-H455
Full text (Publisher's DOI): https://doi.org/10.1152/AJPHEART.00176.2020
To cite this reference: https://hdl.handle.net/10067/1721050151162165141

The Role of Endothelial Autocrine NRG1/ERBB4 Signaling in Cardiac Remodeling

Dugaucquier Lindsey[1]; Feyen Eline[1]; Mateiu Ligia[2]; Bruyns Tine[1]; De Keulenaer Gilles W[1,3,5]; Segers Vincent FM[1,4,5]

[1]Laboratory of Physiopharmacology, University of Antwerp, Universiteitsplein 1, 2610 Antwerp, Belgium

[2]VIB Center for Molecular Neurology, University of Antwerp, Universiteitsplein 1, 2610 Antwerp, Belgium

[3]Department of Cardiology, Middelheim Hospital, Lindendreef 1, 2020 Antwerp, Belgium

[4]Department of Cardiology, University Hospital Antwerp, Wilrijkstraat 10, 2650 Edegem, Belgium

[5]Equally contributed as last author

Running Title: Endothelial ERBB4 and Cardiac Remodeling

Correspondence to Vincent F Segers, Laboratory of Physiopharmacology, University of Antwerp, Universiteitsplein 1, Building T, 2610 Wilrijk, Belgium. Phone: +3232652338. Fax: +3232652412. Email address: vincent.segers@uantwerpen.be

Abstract

Neuregulin-1 (NRG1) is a paracrine growth factor, secreted by cardiac endothelial cells (ECs) in conditions of cardiac overload/injury. The current concept is that the cardiac effects of NRG1 are mediated by activation of ERBB4/ERBB2 receptors on cardiomyocytes. However, recent studies have shown that paracrine effects of NRG1 on fibroblasts and macrophages are equally important. Here, we hypothesize that NRG1 autocrine signaling plays a role in cardiac remodeling.

We generated EC–specific *Erbb4* knockout mice to eliminate endothelial autocrine ERBB4 signaling without affecting paracrine NRG1/ERBB4 signaling in the heart. We first observed no basal cardiac phenotype in these mice up to 32 weeks. We next studied these mice following transverse aortic constriction (TAC), exposure to angiotensin II (Ang II) or myocardial infarction in terms of cardiac performance, myocardial hypertrophy, myocardial fibrosis and capillary density. In general, no major differences between EC–specific *Erbb4* knockout mice and control littermates were observed. However, 8 weeks following TAC both myocardial hypertrophy and fibrosis were attenuated by EC–specific *Erbb4* deletion, albeit these responses were normalized after 20 weeks. Similarly, 4 weeks after Ang II treatment myocardial fibrosis was less pronounced compared to control littermates. These observations were supported by RNA-sequencing experiments on cultured endothelial cells showing that NRG1 controls the expression of various hypertrophic and fibrotic pathways.

Overall, this study shows a role of endothelial autocrine NRG1/ERBB4 signaling in the modulation of hypertrophic and fibrotic responses during *early* cardiac remodeling. This study contributes to understanding the spatio-temporal heterogeneity of myocardial autocrine and paracrine responses following cardiac injury.

Key words

Neuregulin-1, ERBB4, Endothelium, Cardiac remodeling

54 **New and noteworthy**

55 The role of NRG1/ERBB signaling in endothelial cells is not completely understood. Our
56 study contributes to the understanding of spatio-temporal heterogeneity of myocardial
57 autocrine and paracrine responses following cardiac injury, and shows a role of endothelial
58 autocrine NRG1/ERBB4 signaling in the modulation of hypertrophic and fibrotic responses
59 during early cardiac remodeling.

60 **Introduction**

61 Cardiac remodeling—a pathophysiological process with changes in cardiac size, structure,
62 and function—often leads to heart failure in advanced stages. Cardiac remodeling comprises
63 cellular changes in different cell types in the heart—endothelial cells (ECs), cardiomyocytes
64 (CM), fibroblasts, inflammatory cells, and smooth muscle cells. ECs are the most abundant
65 cell type accounting for 45% of the total cardiac cell population and 65% of the non-myocyte
66 population (48, 53). Cross-talk between ECs and other cardiac cells is enabled by a dense
67 capillary network of 3,000–4,000 capillaries/mm^2 (25, 37, 48, 54). CMs depend on ECs not
68 only for oxygenated blood supply but also for paracrine protective signals, mediated through
69 endothelial-derived cardio-active factors. A growing number of these factors has been
70 identified, including nitric oxide (NO), endothelin-1 (ET1), angiotensin II (Ang II),
71 angiopoietins, prostaglandins, and growth factors, like fibroblast growth factor (FGF),
72 vascular endothelial growth factor (VEGF), and neuregulin-1 (NRG1) (6, 7, 25, 34, 37).
73 NRG1 is expressed by ECs and binds in a paracrine manner on erythroblastic leukemia viral
74 oncogene homolog (ERBB)4 and/or ERBB3 (40).
75 NRG1/ERBB signaling is critical during cardiac development (32, 40, 44, 46) and in adult
76 physiology and pathophysiology (11). Conditional *Erbb2*- or *Erbb4*-null mice develop
77 cardiomyopathy and are more sensitive to cardiac stressors, for example ischemia and toxic
78 drugs (20, 23, 44, 45). The NRG1/ERBB system also allows the heart to cope with
79 physiological stress—for example during pregnancy (33). ERBB signaling activates several
80 signaling cascades, including extracellular-signal-regulated kinase 1/2 (ERK1/2), mitogen-
81 activated protein kinase (MAPK), phosphatidylinositol 3-kinase (PI3K)/protein kinase B
82 (AKT), and NO synthase (NOS), to modulate CM growth and survival (10, 16, 30). Increased
83 cardiac expression of NRG1, shedding of NRG1 in the circulation, or activation of cardiac
84 ERBB receptors have been demonstrated in different animal models, including pressure
85 overload–induced left ventricular (LV) hypertrophy (34), ischemia-reperfusion injury (44),
86 rapid ventricular pacing (44) and Ang II–induced arterial hypertension (11, 32, 55). Both

87 preclinical and clinical studies indicate that administration of NRG1 attenuates cardiac
88 remodeling and improves cardiac function in different models of heart failure (19, 21, 27, 50,
89 51).
90 The generally accepted concept is that the cardiac effects of NRG1 are mediated by
91 paracrine activation of ERBB4/ERBB2 receptors on CMs (34, 44). However, recent studies
92 have shown that myeloid-specific deletion of *Erbb4* intensifies myocardial fibrotic responses
93 to Ang II (55). This indicates that paracrine NRG1/ERBB4 signaling in cardiac non-myocytes
94 is equally important. This finding is reinforced by the fact that also fibroblasts express ERBB
95 receptors. Galindo *et al.* showed that GGF2, a secreted neuregulin which binds the ERBB
96 receptors, attenuated myocardial fibrosis, altered extracellular matrix (ECM) structure, and
97 reduced the number of myofibroblasts in a swine model of myocardial infarction (MI). These
98 findings suggest a direct inhibitory effect of GGF2 on cardiac fibroblasts (17).
99 The role of ERBB receptors in ECs is less understood. Previous studies showed the
100 expression of different ERBB receptors (ERBB2, ERBB3, ERBB4) on ECs, and stimulation of
101 ECs with NRG1 induces rapid calcium fluxes, receptor tyrosine phosphorylation, and cell
102 proliferation (34). In addition, it has been shown that stimulation of ERBB2, ERBB3, or
103 ERBB4 receptors by NRG1 results in both *in vitro* and *in vivo* activation of several signaling
104 pathways involved in angiogenesis (26, 28, 52). This effect has been reported to be both
105 dependent and independent of VEGF (26, 52). Kalinowski et al. showed that cytokine-
106 activated matrix metalloproteinase (MMP) cleavage of NRG1 may play an important role in
107 autocrine activation of EC signaling pathways, contributing to its key biological effects (28).
108 Yen et al., on the other hand, showed a modulatory role of ERBB2/ERBB3 heterodimers in
109 the upregulation of VEGF and subsequent in vivo angiogenesis (58). Moreover, endothelial-
110 specific Nrg1 deletion impairs ischemia-induced angiogenesis and decreases flow recovery
111 after femoral artery ligation. This indicates a potential role of NRG1 in vascular disease, like
112 diabetes and coronary artery disease (22). Overall, previous studies have established a role
113 of endothelial NRG1/ERBB signaling in the heart. However, the role of ERBB receptors in
114 ECs during cardiac remodeling remains unclear, and knowledge about the underlying

115 mechanism remains limited. Most endothelium-derived substances like NO and ET-1 have
116 both paracrine and autocrine properties. Endothelial dysfunction results in impairement of
117 these substances and leads to adverse cardiac remodelling and dysfunction (12, 37, 47).
118 Here, we hypothesize that ERBB4-dependent autocrine signaling in ECs plays a role in
119 angiogenesis and cardiac remodeling. Therefore, we generated an EC–specific *Erbb4*
120 knockout (KO) mouse to specifically eliminate endothelial autocrine ERBB4 signaling without
121 affecting paracrine NRG1/ERBB4 signaling in other cardiac cell types. We tested whether
122 this specific conditional deletion of the endothelial ERBB4 receptor, and thus impaired
123 autocrine ERBB4 signaling, changes cardiac remodeling in three different models of cardiac
124 overload/injury.
125
126

127 **Materials and methods**

128 ***Animal models and study design.*** All experiments were approved by the institutional ethics
129 committee of the University of Antwerp and conform to the Guide for the Care and Use of
130 Laboratory Animals, 8th edition, published by the US National Institutes of Health in 2011.
131 Mice were housed in the central animal care facility at the University of Antwerp and were
132 given food and water *ad libitum*. EC–specific deletion of *Erbb4* in mice was examined in
133 three different models of cardiac overload and remodeling: transverse aortic constriction
134 (TAC)–induced pressure overload, Ang II–induced myocardial fibrosis, and left anterior
135 descending artery (LAD) ligation–induced MI. All animals were randomly assigned to
136 treatment groups.

137

138 ***Transgenic mice, endothelial-specific Erbb4 gene deletion.*** Mice with endothelial-specific
139 *Erbb4* gene deletion were generated by crossbreeding tamoxifen-inducible vascular
140 endothelium cadherin5 Cre-recombinase positive (*VE-Cdh5-Cre*$^{+}$) mice
141 (*Cdh5Tg(Cdh5cre/ERT2)CIVE23Mlia; UCLA, Dr. Iruela-Arispe*) with C57BL/6-*Erbb4*$^{F/F}$ mice,
142 carrying LoxP-flanked *Erbb4* alleles (*B6;129-Erbb4tm1Fej/Mmucd, #010439-UCD,MMRRC*)
143 (1, 42). Previously, validation of efficiency and specificity of *VE-Cdh5-Cre* activity has been
144 extensively studied (1, 42, 43). Here, Cre-antibody staining did not show any positivity in CM
145 (data not shown). When crossed with C57BL/6-*Erbb4*$^{F/F}$ mice and treated with tamoxifen (2
146 mg.day^{-1}, for 5 consecutive days) at the age of 6 weeks (42), Cre-mediated recombination
147 results in deletion of *Erbb4* in ECs (*Erbb4*$^{F/F}$ *VE-Cdh5-Cre*$^{+}$ mice). *Erbb4*$^{F/F}$ *VE-Cdh5-Cre*$^{+}$
148 mice treated with vehicle served as controls.

149

150 ***TAC—a model of pressure overload–induced cardiac remodeling.*** TAC was performed
151 in 12-week old mice with endothelial-specific deletion of *Erbb4* and control littermates (n=9–
152 15 per group; *Erbb4*$^{F/F}$ *VE-Cdh5-Cre*$^{+}$ mice with or without tamoxifen treatment). Specifically,
153 adult mice were anesthetized with sevoflurane (3% vol/vol); Sevorane®, Abbott Laboratories,

154 Waver) and ventilated. A partial thoracotomy from the sternum to the second rib was
155 performed. Subsequently, two knots (6.0 silk suture) were tied around the transverse aorta
156 and a blunt 27-gauge needle. Sham-operated animals underwent the same procedure
157 except for the constriction. Post-operative analgesia was administered (buprenorphine; 0.1
158 $mg.kg^{-1}$; i.p.) 8 or 20 weeks after TAC, mice were euthanized and hearts were collected.
159
160 ***Ang II–induced myocardial fibrosis.*** Myocardial fibrosis was induced in 12-week old mice
161 with endothelial-specific deletion of *Erbb4* (n=9–10 per group; *Erbb4*$^{F/F}$ *VE-Cdh5-Cre*$^{+}$ mice
162 with or without tamoxifen treatment) by administration of Ang II (1000 $ng.kg^{-1}.min^{-1}$, Sigma
163 Aldrich) using a micro-osmotic pump (model 1004, Alzet). Post-operative analgesia was
164 administered as above. After 4 weeks of Ang II treatment, mice were euthanized and hearts
165 were collected.
166
167 ***LAD ligation–induced MI.*** MI was induced in 12-week old mice with endothelial-specific
168 deletion of *Erbb4* (n=8–11 per group; *Erbb4*$^{F/F}$ *VE-Cdh5-Cre*$^{+}$ mice with or without tamoxifen
169 treatment). Adult mice were anesthetized with sevoflurane (3% vol/vol), ventilated, and a
170 partial thoracotomy between the fourth and fifth rib was performed. The LAD was ligated 1
171 mm below the left auricle (8-0 Prolene suture; Ethicon, Germany). Sham-operated animals
172 underwent the same procedure, except no ligation was performed. Post-operative analgesia
173 was administered as above. 4 weeks after MI, mice were euthanized and hearts were
174 collected.
175
176 ***Echocardiographic evaluation.*** Transthoracic echocardiography was performed on
177 anesthetized mice (1.5–2.0% vol/vol isoflurane (Forene®, Abbvie)) using a Vevo 2100
178 Imaging System (VisualSonics) equipped with a MS550D probe. A 2D short axis–view of the
179 mid LV was obtained at chordal level using the B-mode (55). In the TAC experiments,
180 ultrasound measurements were performed every 2 weeks. LV internal diameters (LVID;d,
181 LVID;s), interventricular septal wall thickness (IVS;d, IVS;s), and LV posterior wall thickness

182 (LVPW;d, LVPW;s) were measured in diastole (d) and systole (s), respectively, by a single
183 observer in a blinded fashion on three consecutive M-mode cycles. Ejection fraction (EF%)
184 and fractional shortening (FS%) were calculated.
185
186 ***Histological analyses.*** The apical part of the heart was fixed in 4% buffered formalin and
187 embedded in paraffin. Heart sections were stained with Masson's trichrome and laminin
188 (Novus Biologicals) according to the manufacturer's instructions, or with a biotinylated
189 isolectin B4 antibody (IB4; Vector Laboratories), an antibody specific for macrophages
190 (MAC3, PharMingen), or an anti-Cre recombinase antibody (ab190177). Histological images
191 were captured with light microscopy (Olympus SC50, Olympus Stream Motion Software) and
192 analyzed in a blinded fashion using ImageJ 1.52i software. Cardiac interstitial fibrosis and
193 perivascular fibrosis were expressed as the ratio of positively stained fibrotic area (blue
194 staining) to the total cardiac area or vascular lumen area, respectively. Myocardial
195 macrophage content was calculated in the same way. CM cross-sectional area (CSA) was
196 quantified as previously described (55).
197
198 ***Vascular function measurements on isolated aortic segments.*** Thoracic aortae from both
199 control mice and *Erbb4*$^{F/F}$ *VE-Cdh5-Cre*$^{+}$ mice treated with tamoxifen were isolated and cut
200 into 6 segments (n=5 per group; *Erbb4*$^{F/F}$ *VE-Cdh5-Cre*$^{+}$ mice with or without tamoxifen
201 treatment). Segments 2 to 5 were used in an isometric setting and contractile properties were
202 studied as previously described (31).
203
204 ***Human umbilical vein ECs.*** Human umbilical vein ECs (HUVECs; Lonza) were cultured in
205 EC basal medium-2 supplemented with EGM-2 bulletkit (cc-3162) according to the
206 manufacturer's instructions, at 37°C in a humidified 5% CO_2 incubator in collagen-coated
207 (Collagen type I, rat tail, Gibco Life Technologies) culture flasks. Cells were used in passage
208 2 to 10 and 24 h prior to experiments cells were serum-starved (0.1% FBS). Expression of
209 the ERBB4 receptor, phosphorylation of AKT, ERK, and signal transducer and activator of

210 transcription 3 (STAT3) in response to NRG1 stimulation over 1 h and phosphorylation of
211 endothelial NOS (eNOS) in response to NRG1 stimulation over 8 h were determined by
212 Western blotting. In addition, HUVECs were grown in collagen-coated 6-well plates and were
213 exposed to a wound healing scratch assay (35). After scratching, cells were placed in the
214 incubator at 37°C for 18 h with NRG1 (50 $ng.mL^{-1}$) or PBS. After incubation, cells were
215 placed under a phase-contrast microscope (Celena™ S Microscope) and images were
216 captured. Scratch area was measured using Image J software and expressed as % closure
217 after 18 h.
218
219 ***Isolated murine cardiac ECs.*** Cardiac ECs were isolated from hearts of *Erbb4*$^{F/F}$ *VE-Cdh5-*
220 *Cre*$^{+}$ mice treated with tamoxifen or vehicle using Cardiac EC Isolation kit according to
221 manufacturer's instructions (Macs Miltenyi Biotec). Briefly, cardiac ECs were labeled with
222 Cardiac EC Isolation Cocktail and magnetic selection over a MACS LS column. Magnetically
223 retained cardiac ECs were eluted as the positively selected cell fraction. Separated cells
224 were used immediately or cultured in EC basal medium-2 supplemented with EGM-2 bulletkit
225 (cc-3162, Lonza) at 37°C in a humidified 5% CO_2 incubator on collagen coated culture flasks.
226 Purity of ECs was examined by flow cytometry (BD Accuri C6 flow cytometer) using an
227 CD31-APC antibody (murine, 30 $\mu g.mL^{-1}$; Macs Miltenyi Biotec) and expression of the
228 ERBB4 receptor on these isolated ECs was determined by Western blotting.
229
230 ***Primary human cardiac microvascular ECs.*** (HMVECs; Lonza) were cultured in EC basal
231 medium-2 supplemented with clonetic EGM-2 MV bulletkit (cc-3202) at 37°C in a humidified
232 5% CO_2 incubator on collagen coated culture flasks. HMVECs were used in passage 6 and
233 were serum-starved 24 h prior to experiments. HMVECs were stimulated with NRG1 (50
234 $ng.mL^{-1}$) or PBS for 8 or 24 h. After collection of the cells, gene expression was examined by
235 RNA-sequencing.
236

237 ***Aortic Ring Assay.*** The aorta from *Erbb4*$^{F/F}$ *VE-Cdh5-Cre*$^{+}$ mice with or without tamoxifen
238 treatment were isolated and prepared for experiment as described (2). Rings from three
239 separate aortas were used per condition (transgenic mice treated with or without tamoxifen).
240 Rings were incubated with Opti-MEM medium supplemented with NRG1 (50 ng.mL^{-1}) or
241 PBS. Growth medium was changed on day 3 and 5. After 5 days incubation, rings were
242 placed under a phase-contrast microscope (Celena™ S Microscope), images were captured,
243 and microvessel growth was quantified. Each microvessel emerging from the main ring and
244 each individual branch arising from separate vessels was counted. Data was plotted as
245 mean microvessel numbers per ring.
246
247 ***Western blot analysis.*** Following antibodies were used for Western blot analysis: ERBB2
248 (2165, Cell signaling), ERBB3 (SC285, Santa Cruz), ERBB4 (sc283; Santa Cruz), phospho-
249 ERBB2 (sc-81507, Santa Cruz), phospho-ERBB3 (4791, Cell signaling), phospho-ERBB4
250 (4757, Cell signaling), phospho-STAT3 (P-STAT3; 9131, Cell signaling), STAT3 (9132, Cell
251 signaling), phopho-ERK1/2 (P-ERK1/2; 9101, Cell signaling), ERK1/2 (9102, Cell signaling),
252 phospho-AKT (P-AKT; 4058, Cell signaling), AKT (9272, Cell signaling), eNOS (NOS3;
253 PS1177, BD transductions), inducible NOS (iNOS, 13120, Cell signaling), GAPDH (2118
254 (rabbit), 97166 (mouse); Cell signaling). Primary antibodies were incubated overnight at 4°C,
255 diluted at 1:500–1:1000, and detected using an IRDye-conjugated secondary antibody (LI-
256 COR Biosciences). Western blots were analyzed using with the Odyssey Software (LI-COR
257 Biosciences).
258
259 ***Real time-quantitative polymerase chain reaction (RT-qPCR).*** Following TaqMan primers
260 were used for mouse samples (Invitrogen): *Nrg1* (Mm01212130_m1), fibroblast-specific
261 protein 1 (*Fsp1* or *s100a4*) (Mm00803372_g1), *Tgf-β* (Mm01178820_m1), *Vegf* (*Vegfa*,
262 Mm00437306_m1), *Fgf2* (Mm01285715_m1), placental growth factor (*Plgf*,
263 Mm00435613_m1), angiopoietin1 (*Angpt1*, Mm00456503_m1). mRNA expression of the
264 gene of interest was normalized to the expression of β-actin (Mm00607939_s1).

265

266 ***RNA-sequencing.*** Prior to RNA-sequencing, total mRNA was isolated from primary
267 HMVECs by using the mirVana isolation kit (Ambion® by Life Technologies). RNA purity,
268 concentration and quality was measured as previously described (56). Sequence libraries
269 were constructed using QuantSeq 3' mRNA-Seq Library Prep kit for Illumina (Lexogen) and
270 amplified using 15 cycles. RNA-sequencing was performed on NextSeq 500 (Illumina) using
271 NextSeq 500/500 High output Kit v2 (150 cycles), pooling barcoded samples per run.

272

273 ***Bioinformatics analysis.*** The low quality reads were trimmed and the adapter sequences
274 were removed with BBTools (bbduk) using the parameters recommended by Lexogen
275 (GSE150619). The reads were aligned to the human reference genome (ENSEMBL release
276 98) using STAR (13). Gene expression levels were quantified using featureCounts,
277 assembling the uniquely mapped reads at exon level (36). Subsequently, the differential
278 gene expression analyses were performed using DESeq2 R package (39). Correction for
279 multiple testing was performed using the Benjamini-Hochberg false discovery rate (FDR),
280 adjusted p-values < 0.1 were considered statistically significant.

281

282 ***Data analysis and statistics.*** All data are presented as mean ± standard error of mean
283 (SEM). Multiple comparisons of means were performed using one-way ANOVA followed by
284 Dunnett's Multiple Comparison test or two-way ANOVA followed by Bonferroni's Multiple
285 Comparison test. Statistical significance of column factor was defined as $p<0.05, $$p<0.01,
286 $$$p<0.001; statistical significance of row factor was defined as #p<0.05, ##p<0.01,
287 ###p<0.001; statistical significance of post hoc test was defined as *p<0.05, **p<0.01,
288 ***p<0.001. All statistical analyses were performed using GraphPad Prism 6 and IBM SPSS
289 Statistics 23.

290 **Results**

291 **HMVECs and HUVECs are responsive to NRG1 *in vitro*.** ECs are the primary cellular
292 source of NRG1 in the heart, but their responsiveness to NRG1 is incompletely studied (53).
293 Figure 1A demonstrates that HUVECs express ERBB4, ERBB2 and, weakly, ERBB3
294 receptors. NRG1 (50 $ng.mL^{-1}$) induces phosphorylation of both endothelial ERBB4 and
295 ERBB2 receptors 30 minutes after stimulation; endothelial ERBB3 was not activated. In
296 addition, exposure of HUVECs to NRG1 (50 $ng.mL^{-1}$) showed a transient, and statistically
297 insignificant increase in phosphorylation of AKT and ERK1/2 (Fig. 1B; Fig. 1C). STAT3
298 phosphorylation was transiently attenuated (data not shown), whereas total eNOS and iNOS
299 protein levels gradually decreased during 8 h following NRG1 treatment, again these data
300 showed no statistical significance (Fig. 1B; Fig. 1C). We next treated HMVECs for 8 or 24 h
301 with NRG1 and analyzed gene expression levels with RNA-sequencing (n=4 per group).
302 Table S1 and S2 summarize differentially expressed genes by NRG1 in human HMVECs,
303 classified with relation to their function in fibrosis, inflammation, proliferation, growth,
304 differentiation, and angiogenic response. This RNA-sequencing experiment suggests a
305 modulatory role of NRG1 in endothelium-dependent regulation of cardiac hypertrophy,
306 fibrosis, and angiogenesis. Endothelial genes involved in fibrotic responses are mostly
307 upregulated upon NRG1 treatment, whereas inflammatory, hypertrophic and angiogenic
308 genes are both up- and downregulated upon NRG1 treatment. For example, NRG1-induced
309 downregulation in insulin-like growth factor-1 (*Igf1*) could be involved in cardiac hypertrophy
310 (29) and angiogenesis (38). NRG1-induced upregulation in matrix metallopeptidase 2
311 (*Mmp2*) may contribute to changes in ECM (29). Based on these results, we hypothesized
312 that abrogating NRG1-induced endothelial signaling would change cardiac remodeling.
313

314 **Validation of endothelial-specific Erbb4 KO mice.** We created $Erbb4^{F/F}$ VE-Cdh5-Cre^{+}
315 transgenic mice in which endothelial Erbb4 can be conditionally deleted by administration of
316 tamoxifen (Fig. 2A). We validated the model by isolating cardiac ECs from hearts of $Erbb4^{F/F}$

317 VE-Cdh5-Cre^{+} mice treated with tamoxifen or vehicle (EC purity more than 85% in all
318 samples). Western blotting showed that ERBB4 receptor expression was almost completely
319 suppressed by tamoxifen treatment, whereas ERBB2 and the weak ERBB3 expression were
320 not affected (Fig. 2B). EC–specific *Erbb4* KO mice showed no overt phenotypic
321 abnormalities, changes in cardiac function or myocardial histology at baseline. In particular,
322 they showed normal body weight, heart weight/body weight ratio (HW/BW), and
323 echocardiographic parameters (Table S3). Vascular reactivity studies with isolated aortas
324 also showed that EC–specific *Erbb4* deletion induced no changes in vasomotoricity, neither
325 in aortic contractile properties, nor in endothelium-dependent or endothelium-independent
326 aortic dilation (Fig. 2C).
327
328 **NRG1 stimulates EC migration and angiogenesis *in vitro*.** A few studies have shown that
329 NRG1 induces an angiogenic response in ECs (21, 22, 52). Consistent with these findings, in
330 wound healing assays in HUVECs, we found that NRG1 significantly increased migration of
331 ECs compared to PBS after 18 h (Fig. 2D). In addition, in aortic ring assays NRG1
332 significantly increased the number of microvessels sprouting from the main aortic ring from
333 vehicle-treated *Erbb4$^{F/F}$ VE-Cdh5-Cre^{+}* mice. This effect was ERBB4-dependent, since aortic
334 rings from tamoxifen-treated *Erbb4$^{F/F}$ VE-Cdh5-Cre^{+}* mice showed significantly less NRG1-
335 induced microvessel sprouting (Fig. 2E). These data confirm that NRG1 induces an
336 angiogenic response in ECs *in vitro* and demonstrate the role of endothelial ERBB4 in this
337 effect. Based on this finding, we analyzed the effect of *Erbb4* deletion on myocardial capillary
338 density *in vivo* in aging mice (from 12 to 32 weeks). Both control and tamoxifen-treated
339 *Erbb4$^{F/F}$ VE-Cdh5-Cre^{+}* mice showed a small age-dependent capillary rarefaction, but there
340 was no significant difference between groups (Fig. 2F). In addition, myocardial mRNA
341 expression of angiogenic factors, like *Vegf, Fgf2*, *Plgf*, and *Angpt1* did not consistently
342 change by EC–specific *Erbb4* deletion (Fig. 2G). In conclusion, NRG1 induces angiogenic
343 responses *in vitro,* but post-natal induced EC–specific *Erbb4*-deletion did not change

344 baseline myocardial capillary density *in vivo.* Next, we studied the effect of EC–specific
345 *Erbb4* deletion in cardiac remodeling.
346
347 **Effect of endothelial-specific *Erbb4* deletion in three models of cardiac remodeling.**
348 The NRG1/ERBB system is an intrinsic system which is activated by several stimuli including
349 pressure overload, Ang II, or ischemia and attenuates subsequent LV remodeling through
350 NRG1 activity on CMs, inflammatory cells, and fibroblasts (4, 34, 55). Given the fact that
351 NRG1 changes endothelial angiogenic responses (Fig. 2D; Fig. 2E) and its transcriptome
352 (Table S1 and S2), we tested whether *Erbb4* deletion in ECs affected cardiac remodeling
353 induced by different triggers, including pressure overload, Ang II, and MI. We systematically
354 analyzed the effect of EC-specific *Erbb4* deletion during remodeling on LV diameters and
355 performance, LV hypertrophy, myocardial capillary density and myocardial interstitial and
356 perivascular fibrosis.
357
358 ***(i) Effect of endothelial-specific Erbb4 deletion in TAC–induced cardiac overload.*** First,
359 we studied the effects of EC–specific *Erbb4* deletion on pressure overload–induced cardiac
360 hypertrophy by performing TAC in both control mice and tamoxifen-treated *Erbb4*$^{F/F}$ *VE-*
361 *Cdh5-Cre*$^{+}$ mice. TAC is a model of LV remodeling with a time-dependent transition from
362 concentric to eccentric LV hypertrophy, and interstitial and perivascular fibrosis.
363 Figure 3A shows that both control mice and EC–specific *Erbb4* KO mice showed a time-
364 dependent decrease of FS%, and an increase of LVID;d and LVID;s (Table S4, Table S5).
365 Control mice showed significantly increased CM CSA and increased HW/BW both at 8 and
366 20 weeks (Fig. 3B; Fig. 3C). This hypertrophic response was also seen in EC–specific *Erbb4*
367 KO mice at 20 weeks (Fig. 3C), but remained statistically insignificant at 8 weeks (Fig. 3B),
368 suggesting a delay in hypertrophy by EC–specific *Erbb4* deletion.
369 Next, we evaluated the effects of *Erbb4* deletion in ECs on capillary density. No significant
370 effects of TAC on capillary density were observed after 8 weeks (Fig. 4A) and 20 weeks (Fig.
371 4B), neither in control mice, nor in EC–specific *Erbb4* KO mice.

372 With regard to myocardial fibrosis, control mice showed significant increases of interstitial
373 (Fig. 4C; Fig. 4D) and perivascular fibrosis (Fig. 4E; Fig. 4F) both at 8 and 20 weeks after
374 TAC. These fibrotic responses were also seen in EC–specific *Erbb4* KO mice at 20 weeks
375 (Fig. 4D; Fig. 4F). At 8 weeks, however, interstitial fibrosis was statistically milder than control
376 mice (Fig. 4C), suggesting that EC–specific *Erbb4* deletion causes a delay in myocardial
377 fibrosis after TAC. In relation to the delayed fibrotic response, we did not observe altered
378 macrophage density, neither in control mice, nor in EC–specific *Erbb4* KO mice 8 weeks
379 after TAC (Fig. S1).
380
381 ***(ii) Effect of endothelial-specific Erbb4 deletion in Ang II–induced cardiac remodeling.***
382 Next, effects of EC–specific *Erbb4* deletion were examined in a model of Ang II–induced
383 cardiac remodeling. This model is typified by pronounced interstitial and perivascular fibrosis.
384 Both control mice and EC–specific *Erbb4* KO mice were treated with Ang II for 4 weeks.
385 First, despite a significant increase in diastolic septal wall thickness from 0.87±0.02 mm to
386 1.04±0.05 mm ($p<0.05$), CM CSA (Fig. 5A) and HW/BW were only mildly and not significantly
387 increased in control mice (from $5.1*10^{-3}\pm0.3*10^{-3}$ to $5.5*10^{-3}\pm0.2*10^{-3}$; $p>0.05$). EC–specific
388 *Erbb4* deletion did not affect this outcome (increase from $4.9*10^{-3}\pm0.2*10^{-3}$ to $5.3*10^{-}$
389 $^{3}\pm0.2*10^{-3}$; $p>0.05$) (Table S6).
390 As expected, myocardial capillary density was not changed by Ang II treatment neither in
391 control mice nor in EC–specific *Erbb4* KO mice, with no statistically significant differences
392 between groups (Fig. 5B).
393 Next, figure 5C and 5D show the effects of Ang II treatment on cardiac fibrosis. Both
394 interstitial and perivascular fibrosis were significantly increased by Ang II in control and EC–
395 specific *Erbb4* KO mice. However, this fibrotic response was less pronounced in EC–specific
396 *Erbb4* KO mice, and with regard to perivascular fibrosis, significantly less when compared to
397 control mice (Fig. 5D). To further explore this, we analyzed myocardial expression of fibrotic
398 mediators. Figure 5E shows that myocardial *Fsp1* mRNA expression levels were lower in
399 EC–*Erbb4* KO mice compared to control mice, but this remained unaffected by Ang II

400 administration. Also *Tgf-β* mRNA levels were not altered by Ang II treatment. In addition,
401 macrophage density was not altered, neither in control mice, nor in EC–specific *Erbb4* KO
402 mice after 4 weeks of Ang II treatment (Fig. S1).
403
404 ***(iii) Effect of endothelial-specific Erbb4 deletion MI–induced cardiac remodeling.***
405 Finally, we studied the effect of EC–specific *Erbb4* deletion in a model of MI. This model is
406 characterized by LV dilation, decreased myocardial capillary density in the infarcted
407 myocardium and its border zone, and by replacement fibrosis.
408 First, we observed a significant increase in LVID;d after MI in both control mice and EC–
409 specific *Erbb4* KO mice, and this change was not different between both groups (Fig. 6A).
410 Also changes in FS% were not influenced by EC–specific *Erbb4* deletion (Table S7). Figure
411 6B shows that MI induced a significant increase in HW/BW in both control and EC–*Erbb4* KO
412 mice, and also this effect was not different in both groups. CM CSA in the remote zone of
413 infarction after 4 weeks remained unchanged in both groups (Fig. 6A).
414 As expected, myocardial capillary density was significantly reduced in both the infarcted
415 myocardium and its border zone. Again, these changes were not affected by EC–specific
416 *Erbb4* deletion. In the remote zone, no changes in capillary density were observed, neither in
417 control mice, nor in EC–specific *Erbb4* KO mice (Fig. 6C).
418 Finally, with regard to myocardial fibrosis after MI, figure 6D shows that both control mice
419 and EC–specific *Erbb4* KO mice developed increased total myocardial fibrosis. At 4 weeks,
420 there were no statistically significant differences between groups. Of note, at 4 weeks after
421 MI, we did not observe increased interstitial myocardial fibrosis in the remote zone of
422 infarction, neither in control mice, nor in EC–specific *Erbb4* KO mice (data not shown). 4
423 weeks after MI, macrophage density was similar in EC-specific *Erbb4* mice and their control
424 littermates (Fig. S1).
425

426 **Discussion**

427 The major findings of this study are that increased NRG1/ERBB4 signaling in ECs *in vitro*
428 induces angiogenic responses and reprograms several endothelial functions at the genomic
429 level, but that selectively impeding the NRG1/ERBB4 autocrine loop *in vivo* only mildly
430 affects cardiac remodeling following diverse types of myocardial injury.

431 Paracrine communication in the heart is crucial for normal cardiac function, but also plays an
432 important role in cardiac remodeling (34, 44). NRG1 is a paracrine endothelial protein, which
433 binds to ERBB4 on CMs, but also other cell types such as macrophages and fibroblasts (11,
434 17, 55). Here, we examined the role of endothelial autocrine NRG1/ERBB4 receptor
435 signaling during cardiac remodeling. By specifically deleting the ERBB4 receptor on ECs, we
436 selectively eliminated endothelial autocrine ERBB4 signaling without affecting paracrine
437 NRG1/ERBB signaling in other cardiac cell types. Previous studies showed a modulatory role
438 of ERBB2/ERBB3 signaling in angiogenesis *in vivo* (58). Here, we confirmed that NRG1
439 promotes endothelial angiogenic activity *in vitro*, and demonstrated the role of endothelial
440 ERBB4 in this effect. Furthermore, we showed that NRG1 affects a broad range of functional
441 pathways at the genomic level.

442 However, EC–specific *Erbb4* KO mice did not exhibit phenotypic abnormalities at baseline,
443 including cardiac performance or capillary density in aging mice. Also, EC–specific *Erbb4*
444 deletion did not impair *in vitro* vascular vasomotoricity or impair endothelium-dependent
445 relaxation, which was coherent with our observation that NRG1 downregulated endothelial
446 eNOS protein expression in cultured ECs. Although we did not observe a baseline phenotype
447 in mice with EC-specific *Erbb4* deletion, EC-specific *Erbb4* deletion in other organs through
448 the body should be acknowledged and carefully examined in future experiments.

449 By applying three different models of cardiac overload/injury (pressure overload, Ang II, and
450 MI) we observed that the NRG1/ERBB4 autocrine loop has no overt role during cardiac
451 remodeling. For example, EC–specific *Erbb4* deletion had no influence on cardiac
452 performance or capillary density in either of these three models. However, in conditions of

453 pressure overload LV remodeling was delayed by EC–specific *Erbb4* deletion, albeit
454 returning to levels of control mice at 20 weeks after TAC, both in terms of CM hypertrophy
455 and interstitial and perivascular fibrosis. Similar observations were made in mice exposed to
456 4 weeks of Ang II treatment, although in this model longer time points were not studied.
457 Attenuated cardiac hypertrophy and fibrosis by EC–specific deletion of *Erbb4*, albeit
458 temporarily, is a surprising finding because it is in contrast with a previous study in which we
459 showed that specific deletion of *Erbb4* in macrophages increased fibrosis (55). It is also
460 surprising since NRG1/ERBB4 signaling is considered to be a cardioprotective system, and
461 hypertrophy and fibrosis are viewed as maladaptive myocardial responses. However, our
462 data suggest that EC–specific deletion of *Erbb4* only attenuates *early* remodeling. Early
463 myocardial responses following injury are essential to cope with injury and overload and are
464 not maladaptive *per se* (9). It is interesting to notice that these changes are diminished by
465 EC–specific deletion of the ERBB4 receptor, hence that autocrine NRG1/ERBB4 signaling
466 promotes these changes. Therefore, these observations are thought provoking in the
467 understanding of myocardial cell-cell communication during remodeling, and performing
468 future controlled time course experiments could contribute to our understanding of the role of
469 autocrine NRG1/ERBB4 signaling during early cardiac remodeling, and its effects on late
470 cardiac remodeling. Clearly, along with our previous study on specific *Erbb4* deletion in
471 macrophages, this study shows the complexity of intercellular communication during cardiac
472 remodeling, comprising spatio-temporal heterogeneity of myocardial autocrine and paracrine
473 signaling following cardiac overload/injury. Moreover, our study suggests that endothelial
474 NRG1/ERBB4 signaling could contribute to the protective effects of NRG1 during early
475 cardiac remodeling in patients with CHF, but not during late cardiac remodeling. This
476 indicates that the previous observations regarding paracrine anti-fibrotic effects of NRG1
477 remain unaffected (17, 55).
478 What could be the underlying molecular mechanism of this autocrine endothelial modulation
479 of early cardiac remodeling? RNA-sequencing data on altered gene expression in HMVECs,
480 showed that NRG1 upregulated *Skil*, *Pmepa1*, *Thbs1*, *Mmp2*, *Chst11*, *Egr1*, *Egr2*, *Pdgfa*,

481 and *Htra1*. *Skil*, *Pmepa1*, *Thbs1*, *Mmp2*, *Htra1* are positively correlated with mRNA *Tgf-β*
482 levels and associated with fibrotic processes (3, 8, 49) like wound healing (14) and synthesis
483 of ECM (24). A recent study showed that treatment of vascular smooth muscle cells with
484 TGF-β increases *Chst11* mRNA concentrations (41). *Egr1*, a Smad-independent mediator of
485 TGF-β signaling, induces fibrotic processes and is linked to different animal models of
486 fibrosis (5, 57). *Egr2*, on the other hand, could stimulate collagen gene expression and
487 myofibroblast differentiation (15). Gallini *et al.* showed the association of *Pdgfa* with cardiac
488 fibrosis in transgenic mice with overexpression of *Pdgfa* (18). Therefore, NRG1 could
489 activate early cardiac fibrotic responses by activation of these endothelial factors, but further
490 experimental proof for these pathways is currently missing.
491 This study does not address the dimerization partner of ERBB4. ERBB2 is known to be the
492 preferred dimerization partner of ligand-activated ERBB4. However, NRG1 may also induce
493 the formation of ERBB4 homodimers, or ERBB4/ERBB3 heterodimers. However, our *in vitro*
494 and *in vivo* results indicate that expression—and hence activation—of ERBB3 in ECs is low.
495 Currently, it is unknown to what extend EC-specific homotypic (ERBB4/ERBB4) and
496 heterotypic signaling (ERBB2/ERBB4) contribute to the cardioprotective effects of NRG1.
497 Experiments with EC-specific deletion of *Erbb2* could be helpful in answering this question.
498 To summarize, this study shows direct effects of NRG1 on human ECs *in vitro*. EC–specific
499 *Erbb4* deletion in mice attenuated early cardiac responses following pressure overload and
500 Ang II activation, as shown by a delayed hypertrophic and fibrotic response. EC–specific
501 *Erbb4* deletion did not influence capillary density or change cardiac performance *in vivo*.
502 These data contribute to our understanding of myocardial cell-cell communication during
503 cardiac remodeling and to the role of autocrine NRG1/ERBB4 signaling specifically, and
504 provides new avenues for future research.
505
506

507 **Author's Contributions**

508 LD, EF, VFMS and GWDK participated in the design of the studies, contributed to the
509 interpretation of the results and prepared the manuscript. Animal experiments were
510 performed by LD. Cell culture experiments by LD, EF and TB. Hemodynamic measurements,
511 molecular assays, histological examination and statistical data analysis were performed by
512 LD and TB. RNA-sequencing experiments and analysis was performed by LD and LM. Flow
513 cytometry was performed by LD. All authors read and approved the final manuscript.

514

515 **Acknowledgments**

516 We would like to thank Rita Van Den Bossche and the Neuromics Support Facility (University
517 of Antwerp) for technical support. This work was supported by a DocPro Ph.D. fellowship (to
518 LD, PID33081), a Dehousse Ph.D. fellowship (to EF), a IOF/SBO research grant (PID34923),
519 and a GOA grant (PID36444) of the University of Antwerp; by a Senior Clinical Investigator
520 fellowship (to VFS) and research grants of the Fund for Scientific Research Flanders
521 (Application numbers 1842219N, G021019N, and G021420N); by a research grant of
522 ERA.Net RUS Plus (2018, Project Consortium 278).

523

524 **Disclosures**

525 No conflicts of interest, financial or otherwise, are declared by the authors.

526

527 **References**

528 1. Alva JA, Zovein AC, Monvoisin A, Murphy T, Salazar A, Harvey NL, et al. VE-
529 Cadherin-Cre-recombinase transgenic mouse: a tool for lineage analysis and gene deletion
530 in endothelial cells. Developmental dynamics : an official publication of the American
531 Association of Anatomists. 2006;235(3):759-67.
532 2. Baker M, Robinson SD, Lechertier T, Barber PR, Tavora B, D'amico G, et al. Use of
533 the mouse aortic ring assay to study angiogenesis. Nature protocols. 2012;7(1):89.
534 3. Beaufort N, Scharrer E, Kremmer E, Lux V, Ehrmann M, Huber R, et al. Cerebral
535 small vessel disease-related protease HtrA1 processes latent TGF-β binding protein 1 and
536 facilitates TGF-β signaling. Proceedings of the National Academy of Sciences of the United
537 States of America. 2014;111(46):16496-501.
538 4. Bersell K, Arab S, Haring B, Kuhn B. Neuregulin1/ErbB4 signaling induces
539 cardiomyocyte proliferation and repair of heart injury. Cell. 2009;138(2):257-70.
540 5. Bhattacharyya S, Wu M, Fang F, Tourtellotte W, Feghali-Bostwick C, Varga J. Early
541 growth response transcription factors: key mediators of fibrosis and novel targets for anti-
542 fibrotic therapy. Matrix Biol. 2011;30(4):235-42.
543 6. Brutsaert DL. Role of endocardium in cardiac overloading and failure. European heart
544 journal. 1990;11 Suppl G:8-16.
545 7. Brutsaert DL, Fransen P, Andries LJ, De Keulenaer GW, Sys SU. Cardiac
546 endothelium and myocardial function. Cardiovascular Research. 1998;38(2):281-90.
547 8. Cao Y, Agarwal R, Dituri F, Lupo L, Trerotoli P, Mancarella S, et al. NGS-based
548 transcriptome profiling reveals biomarkers for companion diagnostics of the TGF-β receptor
549 blocker galunisertib in HCC. Cell death & disease. 2017;8(2):e2634-e.
550 9. Cohn JN, Ferrari R, Sharpe N. Cardiac remodeling—concepts and clinical
551 implications: a consensus paper from an international forum on cardiac remodeling. Journal
552 of the American College of Cardiology. 2000;35(3):569-82.
553 10. De Keulenaer GW, Doggen K, Lemmens K. The vulnerability of the heart as a
554 pluricellular paracrine organ: lessons from unexpected triggers of heart failure in targeted
555 ErbB2 anticancer therapy. Circulation research. 2010;106(1):35-46.
556 11. De Keulenaer GW, Feyen E, Dugaucquier L, Shakeri H, Shchendrygina A, Belenkov
557 YN, et al. Mechanisms of the Multitasking Endothelial Protein NRG-1 as a Compensatory
558 Factor During Chronic Heart Failure. Circ Heart Fail. 2019;12(10):e006288.
559 12. De Keulenaer GW, Segers VFM, Zannad F, Brutsaert DL. The future of pleiotropic
560 therapy in heart failure. Lessons from the benefits of exercise training on endothelial function.
561 European journal of heart failure. 2017;19(5):603-14.
562 13. Dobin A, Davis CA, Schlesinger F, Drenkow J, Zaleski C, Jha S, et al. STAR: ultrafast
563 universal RNA-seq aligner. Bioinformatics (Oxford, England). 2013;29(1):15-21.
564 14. Faler BJ, Macsata RA, Plummer D, Mishra L, Sidawy AN. Transforming growth factor-
565 beta and wound healing. Perspectives in vascular surgery and endovascular therapy.
566 2006;18(1):55-62.
567 15. Fang F, Ooka K, Bhattacharyya S, Wei J, Wu M, Du P, et al. The early growth
568 response gene Egr2 (Alias Krox20) is a novel transcriptional target of transforming growth
569 factor-β that is up-regulated in systemic sclerosis and mediates profibrotic responses. Am J
570 Pathol. 2011;178(5):2077-90.
571 16. Fuller SJ, Sivarajah K, Sugden PH. ErbB receptors, their ligands, and the
572 consequences of their activation and inhibition in the myocardium. Journal of Molecular and
573 Cellular Cardiology. 2008;44(5):831-54.
574 17. Galindo CL, Kasasbeh E, Murphy A, Ryzhov S, Lenihan S, Ahmad FA, et al. Anti-
575 remodeling and anti-fibrotic effects of the neuregulin-1beta glial growth factor 2 in a large
576 animal model of heart failure. Journal of the American Heart Association. 2014;3(5):e000773.
577 18. Gallini R, Lindblom P, Bondjers C, Betsholtz C, Andrae J. PDGF-A and PDGF-B
578 induces cardiac fibrosis in transgenic mice. Experimental cell research. 2016;349(2):282-90.

579 19. Gao R, Zhang J, Cheng L, Wu X, Dong W, Yang X, et al. A Phase II, randomized,
580 double-blind, multicenter, based on standard therapy, placebo-controlled study of the efficacy
581 and safety of recombinant human neuregulin-1 in patients with chronic heart failure. Journal
582 of the American College of Cardiology. 2010;55(18):1907-14.
583 20. Garcia-Rivello H, Taranda J, Said M, Cabeza-Meckert P, Vila-Petroff M, Scaglione J,
584 et al. Dilated cardiomyopathy in Erb-b4-deficient ventricular muscle. American journal of
585 physiology Heart and circulatory physiology. 2005;289(3):H1153-60.
586 21. Gui C, Zeng ZY, Chen Q, Luo YW, Li L, Chen LL. Neuregulin-1 Promotes Myocardial
587 Angiogenesis in the Rat Model of Diabetic Cardiomyopathy. Cell Physiol Biochem.
588 2018;46(6):2325-34.
589 22. Hedhli N, Dobrucki LW, Kalinowski A, Zhuang ZW, Wu X, Russell RR, et al.
590 Endothelial-derived neuregulin is an important mediator of ischaemia-induced angiogenesis
591 and arteriogenesis. Cardiovascular research. 2012;93(3):516-24.
592 23. Hedhli N, Huang Q, Kalinowski A, Palmeri M, Hu X, Russell RR, et al. Endothelium-
593 derived neuregulin protects the heart against ischemic injury. Circulation.
594 2011;123(20):2254-62.
595 24. Hocevar BA, Howe PH. Analysis of TGF-beta-mediated synthesis of extracellular
596 matrix components. Methods in molecular biology (Clifton, NJ). 2000;142:55-65.
597 25. Hsieh PCH, Davis ME, Lisowski LK, Lee RT. Endothelial-Cardiomyocyte Interactions
598 in Cardiac Development and Repair. Annual Review of Physiology. 2006;68:51-66.
599 26. Iivanainen E, Paatero I, Heikkinen SM, Junttila TT, Cao R, Klint P, et al. Intra- and
600 extracellular signaling by endothelial neuregulin-1. Experimental cell research.
601 2007;313(13):2896-909.
602 27. Jabbour A, Hayward CS, Keogh AM, Kotlyar E, McCrohon JA, England JF, et al.
603 Parenteral administration of recombinant human neuregulin-1 to patients with stable chronic
604 heart failure produces favourable acute and chronic haemodynamic responses. European
605 journal of heart failure. 2011;13(1):83-92.
606 28. Kalinowski A, Plowes NJ, Huang Q, Berdejo-Izquierdo C, Russell RR, Russell KS.
607 Metalloproteinase-dependent cleavage of neuregulin and autocrine stimulation of vascular
608 endothelial cells. FASEB journal : official publication of the Federation of American Societies
609 for Experimental Biology. 2010;24(7):2567-75.
610 29. Kehat I, Molkentin JD. Molecular pathways underlying cardiac remodeling during
611 pathophysiological stimulation. Circulation. 2010;122(25):2727-35.
612 30. Kuramochi Y, Guo X, Sawyer DB. Neuregulin activates erbB2-dependent src/FAK
613 signaling and cytoskeletal remodeling in isolated adult rat cardiac myocytes. J Mol Cell
614 Cardiol. 2006;41(2):228-35.
615 31. Leloup AJA, De Moudt S, Van Hove CE, Dugaucquier L, Vermeulen Z, Segers VFM,
616 et al. Short-Term Angiotensin II Treatment Affects Large Artery Biomechanics and Function
617 in the Absence of Small Artery Alterations in Mice. Front Physiol. 2018;9:582.
618 32. Lemmens K, Doggen K, De Keulenaer GW. Role of neuregulin-1/ErbB signaling in
619 cardiovascular physiology and disease: implications for therapy of heart failure. Circulation.
620 2007;116(8):954-60.
621 33. Lemmens K, Doggen K, De Keulenaer GW. Activation of the neuregulin/ErbB system
622 during physiological ventricular remodeling in pregnancy. American Journal of Physiology-
623 Heart and Circulatory Physiology. 2011;300(3):H931-H42.
624 34. Lemmens K, Segers VF, Demolder M, De Keulenaer GW. Role of neuregulin-1/ErbB2
625 signaling in endothelium-cardiomyocyte cross-talk. J Biol Chem. 2006;281(28):19469-77.
626 35. Liang CC, Park AY, Guan JL. In vitro scratch assay: a convenient and inexpensive
627 method for analysis of cell migration in vitro. Nature protocols. 2007;2(2):329-33.
628 36. Liao Y, Smyth GK, Shi W. featureCounts: an efficient general purpose program for
629 assigning sequence reads to genomic features. Bioinformatics. 2014;30(7):923-30.
630 37. Lim SL, Lam CS, Segers VF, Brutsaert DL, De Keulenaer GW. Cardiac endothelium-
631 myocyte interaction: clinical opportunities for new heart failure therapies regardless of
632 ejection fraction. European heart journal. 2015;36(31):2050-60.

633 38. Lin S, Zhang Q, Shao X, Zhang T, Xue C, Shi S, et al. IGF-1 promotes angiogenesis
634 in endothelial cells/adipose-derived stem cells co-culture system with activation of PI3K/Akt
635 signal pathway. Cell proliferation. 2017;50(6).
636 39. Love MI, Huber W, Anders S. Moderated estimation of fold change and dispersion for
637 RNA-seq data with DESeq2. Genome Biol. 2014;15(12):550.
638 40. Mendes-Ferreira P, De Keulenaer GW, Leite-Moreira AF, Bras-Silva C. Therapeutic
639 potential of neuregulin-1 in cardiovascular disease. Drug discovery today. 2013;18(17-
640 18):836-42.
641 41. Mohamed R, Dayati P, Mehr RN, Kamato D, Seif F, Babaahmadi-Rezaei H, et al.
642 Transforming growth factor-β1 mediated CHST11 and CHSY1 mRNA expression is ROS
643 dependent in vascular smooth muscle cells. J Cell Commun Signal. 2019;13(2):225-33.
644 42. Monvoisin A, Alva JA, Hofmann JJ, Zovein AC, Lane TF, Iruela-Arispe ML. VE-
645 cadherin-CreERT2 transgenic mouse: a model for inducible recombination in the
646 endothelium. Developmental dynamics : an official publication of the American Association of
647 Anatomists. 2006;235(12):3413-22.
648 43. Oberlin E, El Hafny B, Petit-Cocault L, Souyri M. Definitive human and mouse
649 hematopoiesis originates from the embryonic endothelium: a new class of HSCs based on
650 VE-cadherin expression. Int J Dev Biol. 2010;54(6-7):1165-73.
651 44. Odiete O, Hill MF, Sawyer DB. Neuregulin in Cardiovascular Development and
652 Disease. Circulation research. 2012;111(10):1376-85.
653 45. Ozcelik C, Erdmann B, Pilz B, Wettschureck N, Britsch S, Hubner N, et al. Conditional
654 mutation of the ErbB2 (HER2) receptor in cardiomyocytes leads to dilated cardiomyopathy.
655 Proceedings of the National Academy of Sciences of the United States of America.
656 2002;99(13):8880-5.
657 46. Parodi EM, Kuhn B. Signalling between microvascular endothelium and
658 cardiomyocytes through neuregulin. Cardiovascular research. 2014;102(2):194-204.
659 47. Paulus WJ, Tschope C. A novel paradigm for heart failure with preserved ejection
660 fraction: comorbidities drive myocardial dysfunction and remodeling through coronary
661 microvascular endothelial inflammation. Journal of the American College of Cardiology.
662 2013;62(4):263-71.
663 48. Pinto AR, Ilinykh A, Ivey MJ, Kuwabara JT, D'Antoni ML, Debuque R, et al. Revisiting
664 Cardiac Cellular Composition. Circulation research. 2016;118(3):400-9.
665 49. Pohlers D, Brenmoehl J, Loffler I, Muller CK, Leipner C, Schultze-Mosgau S, et al.
666 TGF-beta and fibrosis in different organs - molecular pathway imprints. Biochimica et
667 biophysica acta. 2009;1792(8):746-56.
668 50. Rohrbach S, Niemann B, Silber RE, Holtz J. Neuregulin receptors erbB2 and erbB4 in
669 failing human myocardium -- depressed expression and attenuated activation. Basic Res
670 Cardiol. 2005;100(3):240-9.
671 51. Rohrbach S, Yan X, Weinberg EO, Hasan F, Bartunek J, Marchionni MA, et al.
672 Neuregulin in cardiac hypertrophy in rats with aortic stenosis. Differential expression of erbB2
673 and erbB4 receptors. Circulation. 1999;100(4):407-12.
674 52. Russell KS, Stern DF, Polverini PJ, Bender JR. Neuregulin activation of ErbB
675 receptors in vascular endothelium leads to angiogenesis. American Journal of Physiology-
676 Heart and Circulatory Physiology. 1999;277(6):H2205-H11.
677 53. Segers VFM, Brutsaert DL, De Keulenaer GW. Cardiac Remodeling: Endothelial Cells
678 Have More to Say Than Just NO. Front Physiol. 2018;9:382.
679 54. Tirziu D, Giordano FJ, Simons M. Cell communications in the heart. Circulation.
680 2010;122(9):928-37.
681 55. Vermeulen Z, Hervent AS, Dugaucquier L, Vandekerckhove L, Rombouts M, Beyens
682 M, et al. Inhibitory actions of the NRG-1/ErbB4 pathway in macrophages during tissue
683 fibrosis in the heart, skin, and lung. American journal of physiology Heart and circulatory
684 physiology. 2017;313(5):H934-H45.
685 56. Vermeulen Z, Mateiu L, Dugaucquier L, De Keulenaer GW, Segers VFM. Cardiac
686 endothelial cell transcriptome in neonatal, adult, and remodeling hearts. Physiological
687 genomics. 2019;51(6):186-96.

688 57. Wu M, Varga J. In perspective: murine models of scleroderma. Current rheumatology
689 reports. 2008;10(3):173-82.
690 58. Yen L, Benlimame N, Nie Z-R, Xiao D, Wang T, Al Moustafa A-E, et al. Differential
691 regulation of tumor angiogenesis by distinct ErbB homo- and heterodimers. Mol Biol Cell.
692 2002;13(11):4029-44.
693

694

695 **Figure legends**

696 **Figure 1: HUVECs are responsive to NRG1 in vitro.** A: Total and phosphorylated protein
697 levels of ERBB4, ERBB2, and ERBB3 receptors in Human Umbilical Vein ECs (HUVECs)
698 were analyzed using Western blot analysis (3 repeats). B: Protein levels of (P-)AKT, (P-
699)ERK1/2, and total eNOS and iNOS in HUVECs were determined using Western blot
700 analysis after 0 to 60 min (AKT, ERK) and after 0 to 8 h (eNOS, iNOS) stimulation with
701 NRG1. C: Protein levels of (P-)AKT, (P-)ERK1/2, and total eNOS and iNOS in HUVECs were
702 quantified using Odyssey Software (2 repeats). Results are expressed as mean ± SEM.
703

704 **Figure 2: Phenotypic characterization of endothelial-specific Erbb4 KO mice and**
705 **angiogenic properties of NRG1.** A: Creation of tamoxifen-inducible Erbb4$^{F/F}$ VE-Cdh5-Cre^{+}
706 mice (EC-KO). B: Western blot analysis of ERBB4, ERBB2, and ERBB3 protein levels in
707 isolated endothelial cells (EC) of Erbb4$^{F/F}$ VE-Cdh5-Cre^{+} mice treated with tamoxifen (EC-
708 KO) or vehicle (EC-CTR) (2 repeats). C: Isometric force (%) of isolated aortic segments of
709 both tamoxifen-treated Erbb4$^{F/F}$ VE-Cdh5-Cre^{+} and control mice after phenylephrine (PE),
710 acetylcholine (Ach) or DEANO administration (n=5 per group). D: Representative bright field
711 images of cultured HUVECs in a scratch wound-healing assay (n=3; 3 repeats), and
712 quantification of % closure 18 h after scratching with vehicle (PBS) or NRG1 (50 ng.mL^{-1})
713 treatment. E: Representative bright field images of aortic rings from both control mice and
714 tamoxifen-treated Erbb4$^{F/F}$ VE-Cdh5-Cre^{+} mice (n=20 rings per condition; 3 repeats) after
715 treatment with PBS or NRG1 (50 ng.mL^{-1}), and quantification of mean number of microvessel
716 sprouts per ring (indicated by →). F: Quantification of capillary density (capillaries/mm^{2}) of
717 control mice and tamoxifen-treated Erbb4$^{F/F}$ VE-Cdh5-Cre^{+} mice at baseline (n=9 per time
718 point). G: Fold induction of mRNA expression of Vefg, Fgf2, Plgf, Angpt1 in heart samples of
719 control mice versus tamoxifen-treated Erbb4$^{F/F}$ VE-Cdh5-Cre^{+} mice at baseline over a time
720 course of 32 weeks (n=9 per time point). Results are expressed relative to control (sham).
721 There was a significant effect of age on capillary density and Vegf, Fgf2, and Angpt1 mRNA

722 (not indicated on the figure). Post hoc test (Dunnett's Multiple Comparison test (D);
723 Bonferroni's Multiple Comparison test (E;F)): *p<0.05, **p<0.01, ***p<0.001. Results are
724 expressed as mean ± SEM (C); results are expressed as Box-Whiskers-plots (D-G).
725
726 **Figure 3: Endothelial-specific Erbb4 deletion did not affect cardiac performance and a**
727 **delayed hypertrophic response was observed 8 to 20 weeks after TAC.** A:
728 Echocardiographic measurement of fractional shortening (FS%) and left ventricular internal
729 diameter in diastole (LVID;d) in control mice (EC-CTR) and tamoxifen-treated Erbb4$^{F/F}$ VE-
730 Cdh5-Cre^{+} mice (EC-KO) with a follow-up of 20 weeks after TAC (n=9–15 per group); *
731 indicates a significant difference between EC-KO–sham and EC-KO–TAC (post hoc test). B:
732 Representative laminin stained heart sections (n=9–15 per group; scale bar=100 μm), and
733 quantification of CM CSA (μm^2) and HW/BW (g/g) of control mice and EC–specific Erbb4 KO
734 mice 8 weeks after TAC. C: Representative laminin stained heart sections (n=9–15 per
735 group; scale bar=100 μm), and quantification of CM CSA (μm^2) and HW/BW (g/g) of control
736 mice and EC–specific Erbb4 KO mice 20 weeks after TAC. Statistical significance of two-way
737 ANOVA is defined as $p<0.05, $$p<0.01, $$$p<0.001, indicating a significant overall effect
738 of TAC relative to sham regardless of EC–specific Erbb4 deletion; Post hoc test (Bonferroni's
739 Multiple Comparison test): *p<0.05, **p<0.01, ***p<0.001; Results are expressed as mean ±
740 SEM (A); results are expressed as Box-Whiskers-plots (B-C).
741
742 **Figure 4: Endothelial-specific Erbb4 deletion did not affect capillary density, but alters**
743 **fibrotic responses 8 to 20 weeks after TAC.** A, B: Representative IB4 stained heart
744 sections (n=9–15; scale bar=100 μm), and quantification of capillary density (capillaries/mm^2)
745 of control mice (EC-CTR) and tamoxifen-treated Erbb4$^{F/F}$ VE-Cdh5-Cre^{+} mice (EC-KO) 8
746 weeks after TAC (A) and 20 weeks after TAC (B). C, D: Representative Masson's Trichrome
747 stained heart sections (n=9–15; scale bar=100 μm), and quantification of cardiac interstitial
748 fibrosis of control mice versus tamoxifen-treated Erbb4$^{F/F}$ VE-Cdh5-Cre^{+} mice 8 weeks after
749 TAC (C) and 20 weeks after TAC (D). E, F: Representative Masson's Trichrome stained

750 heart sections (n=9–15; scale bar=100 μm), and quantification of perivascular fibrosis of
751 control mice versus tamoxifen-treated Erbb4$^{F/F}$ VE-Cdh5-Cre^{+} mice 8 weeks after TAC (E)
752 and 20 weeks after TAC (F). Statistical significance of two-way ANOVA is defined as
753 $$p<0.01, $$$p<0.001, indicating a significant overall effect of TAC relative to sham
754 regardless of EC–specific Erbb4 deletion, and as #p<0.05, indicating a significant overall
755 effect of KO relative to CTR regardless the procedure; Post hoc test (Bonferroni's Multiple
756 Comparison test): *p<0.05, **p<0.01, ***p<0.001; Results are expressed as Box-Whiskers-
757 plots.
758
759 **Figure 5: Endothelial-specific Erbb4 deletion did not affect hypertrophic responses or**
760 **capillary density, but attenuated cardiac fibrosis after 4 weeks of Ang II treatment.** A:
761 Representative laminin stained heart sections (n=9–10 per group; scale bar=100 μm), and
762 quantification of CM CSA (μm^2) of control mice (EC-CTR) and EC–specific Erbb4 KO mice
763 (EC-KO) after 4 weeks of Ang II treatment. B: Representative IB4 stained heart sections
764 (n=9–10; scale bar=100 μm), and quantification of capillary density (capillaries/mm^2) of
765 control mice and tamoxifen-treated Erbb4$^{F/F}$ VE-Cdh5-Cre^{+} mice after 4 weeks of Ang II
766 treatment. C: Representative Masson's Trichrome stained heart sections (n=9–10 per group;
767 scale bar=100 μm), and quantification of cardiac interstitial fibrosis in hearts of control mice
768 versus tamoxifen-treated Erbb4$^{F/F}$ VE-Cdh5-Cre^{+} mice after 4 weeks of Ang II treatment. D:
769 Representative Masson's Trichrome stained heart sections (n=9–10 per group; scale
770 bar=100 μm), and quantification of perivascular fibrosis in hearts of control mice versus
771 tamoxifen-treated Erbb4$^{F/F}$ VE-Cdh5-Cre^{+} mice after 4 weeks of Ang II treatment. E: Fold
772 induction of mRNA expression of Fsp1, and Tgf-β, in heart samples of control mice versus
773 tamoxifen-treated Erbb4$^{F/F}$ VE-Cdh5-Cre^{+} mice after 4 weeks of Ang II treatment 5 (n=9–10
774 per group). Results are expressed relative to control (sham). Statistical significance of two-
775 way ANOVA is defined as $$$p<0.001, indicating a significant overall effect of Ang II relative
776 to sham regardless of EC–specific Erbb4 deletion, and as #p<0.05, ##p<0.01, indicating a
777 significant overall effect of KO relative to CTR regardless the procedure; Post hoc test

778 (Bonferroni's Multiple Comparison test): **p<0.01, ***p<0.001; Results are expressed as
779 Box-Whiskers-plots.
780
781 **Figure 6: Endothelial-specific Erbb4 deletion did not affect cardiac performance,**
782 **hypertrophy, capillary density, or fibrosis in an in vivo MI model.** A: Echocardiographic
783 measurements of control mice (EC-CTR) and tamoxifen-treated Erbb4$^{F/F}$ VE-Cdh5-Cre^{+} mice
784 (EC-KO) with a follow-up of 4 weeks after MI (n=8–11 per group). Left ventricular internal
785 diameter in diastole (LVID;d) is shown. B: Representative laminin stained heart sections
786 (n=8–11 per group; scale bar=100 μm), and quantification of CM CSA (μm^2) and HW/BW
787 (g/g) of control mice and tamoxifen-treated Erbb4$^{F/F}$ VE-Cdh5-Cre^{+} mice 4 weeks after MI. C:
788 Quantification of IB4 stained heart sections (n=8–11), capillary density (capillaries/mm^2) of
789 both control mice and tamoxifen-treated Erbb4$^{F/F}$ VE-Cdh5-Cre^{+} mice was analyzed 4 weeks
790 after MI in the infarcted zone, border zone, and remote zone. D: Representative Masson's
791 Trichrome stained heart sections (n=8–11 per group; scale bar=1000 μm), and quantification
792 of cardiac fibrosis of control mice versus tamoxifen-treated Erbb4$^{F/F}$ VE-Cdh5-Cre^{+} mice 4
793 weeks after MI. Statistical significance of two-way ANOVA is defined as $p<0.05,
794 $$$p<0.001, indicating a significant overall effect of LAD relative to sham regardless of EC–
795 specific Erbb4 deletion; Post hoc test (Bonferroni's Multiple Comparison test): **p<0.01,
796 ***p<0.001; Results are as mean ± SEM (A); results are expressed as Box-Whiskers-plots
797 (B-D).
798
799 **Supplemental Material Link**
800 https://doi.org/10.5281/zenodo.3925113
801

Figure 1

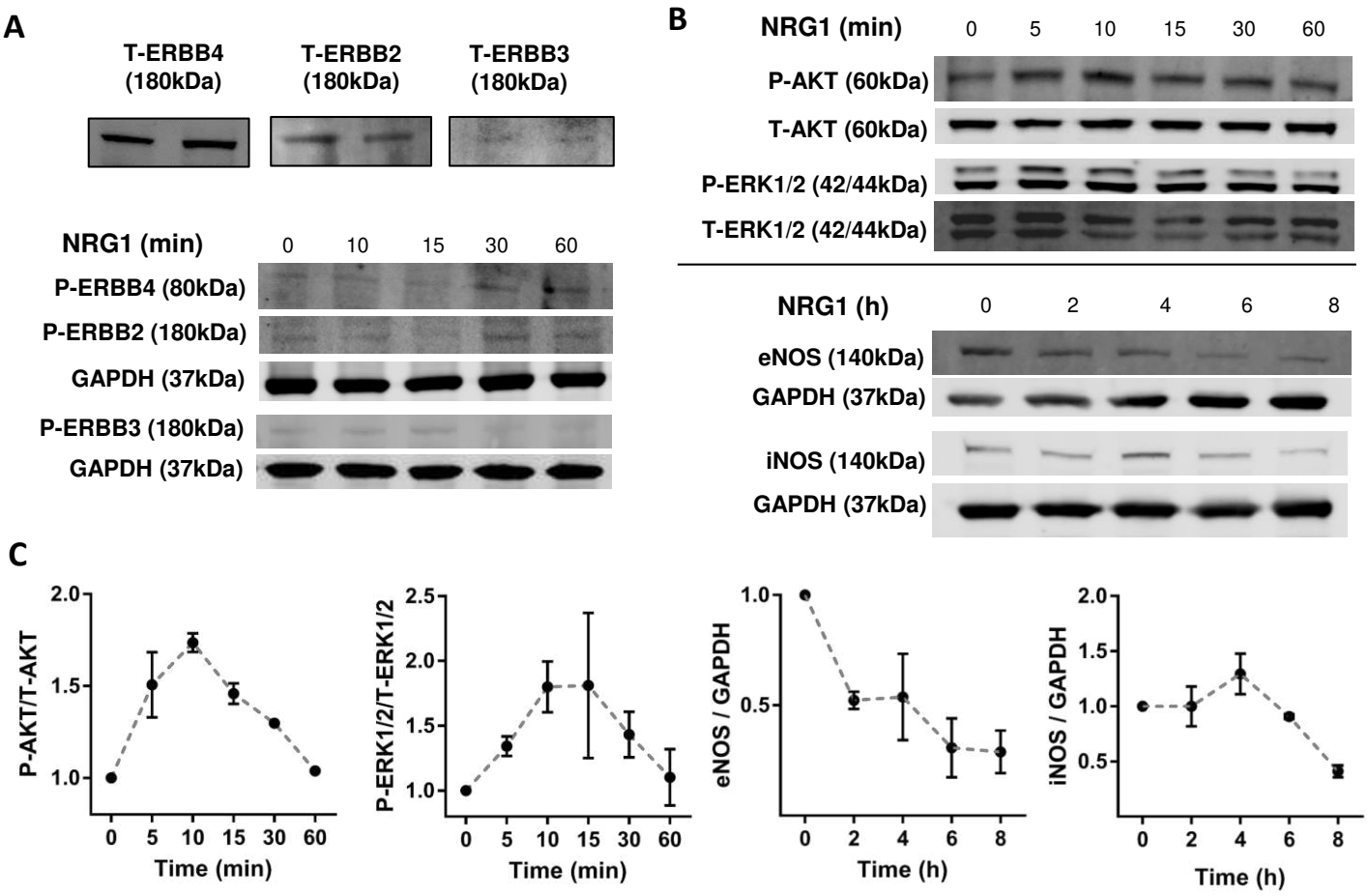

Figure 2

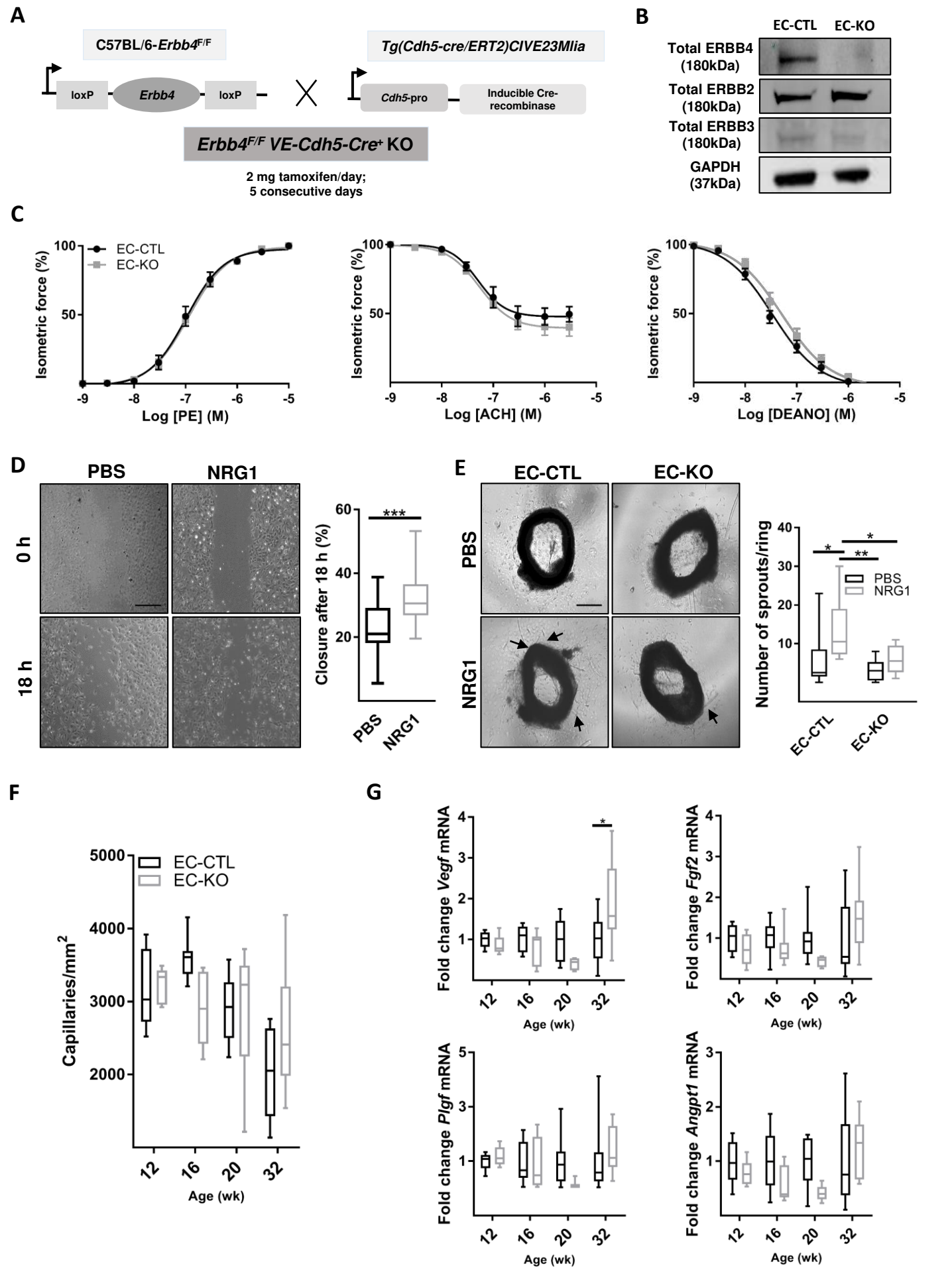

Figure 3

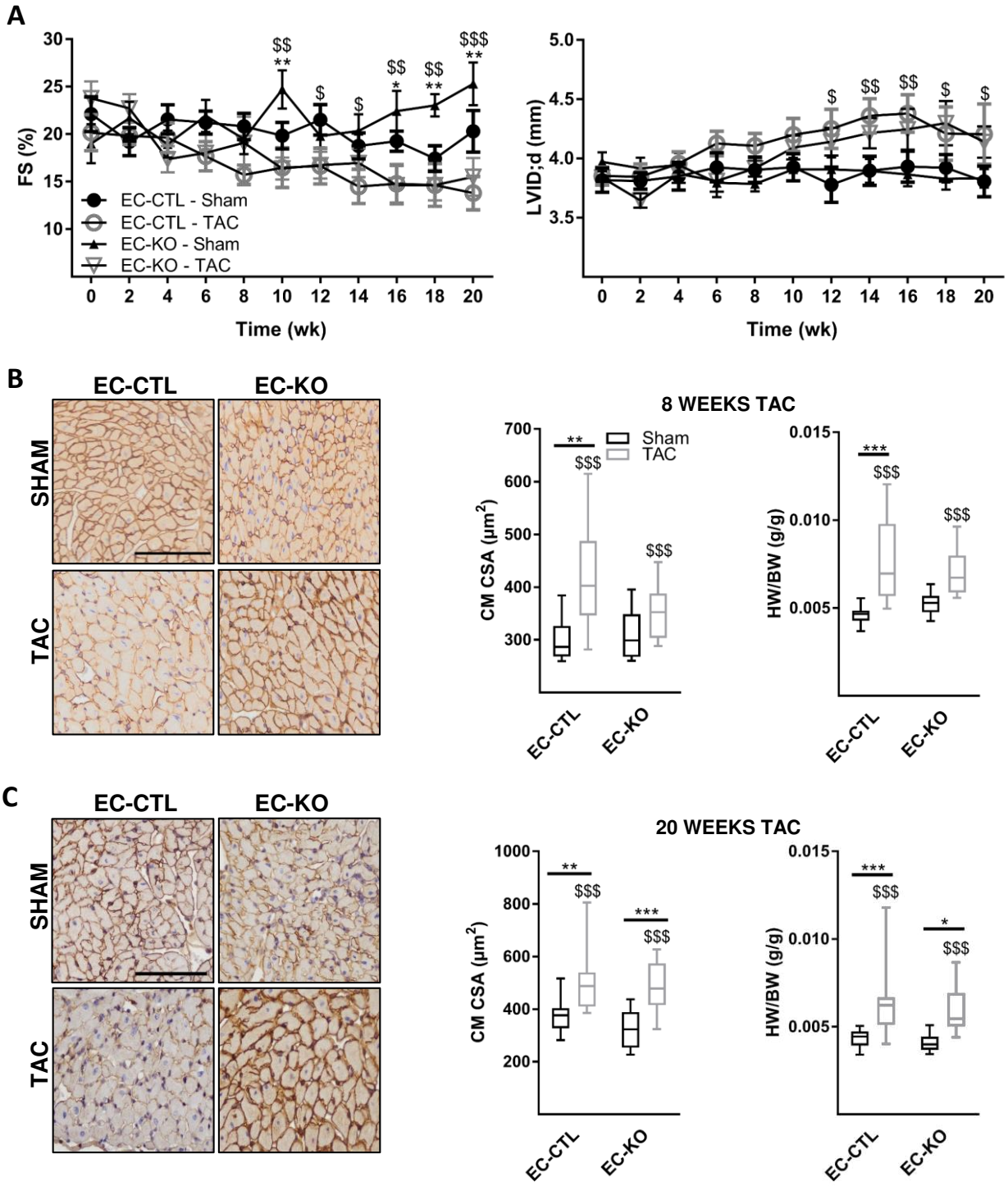

Figure 4

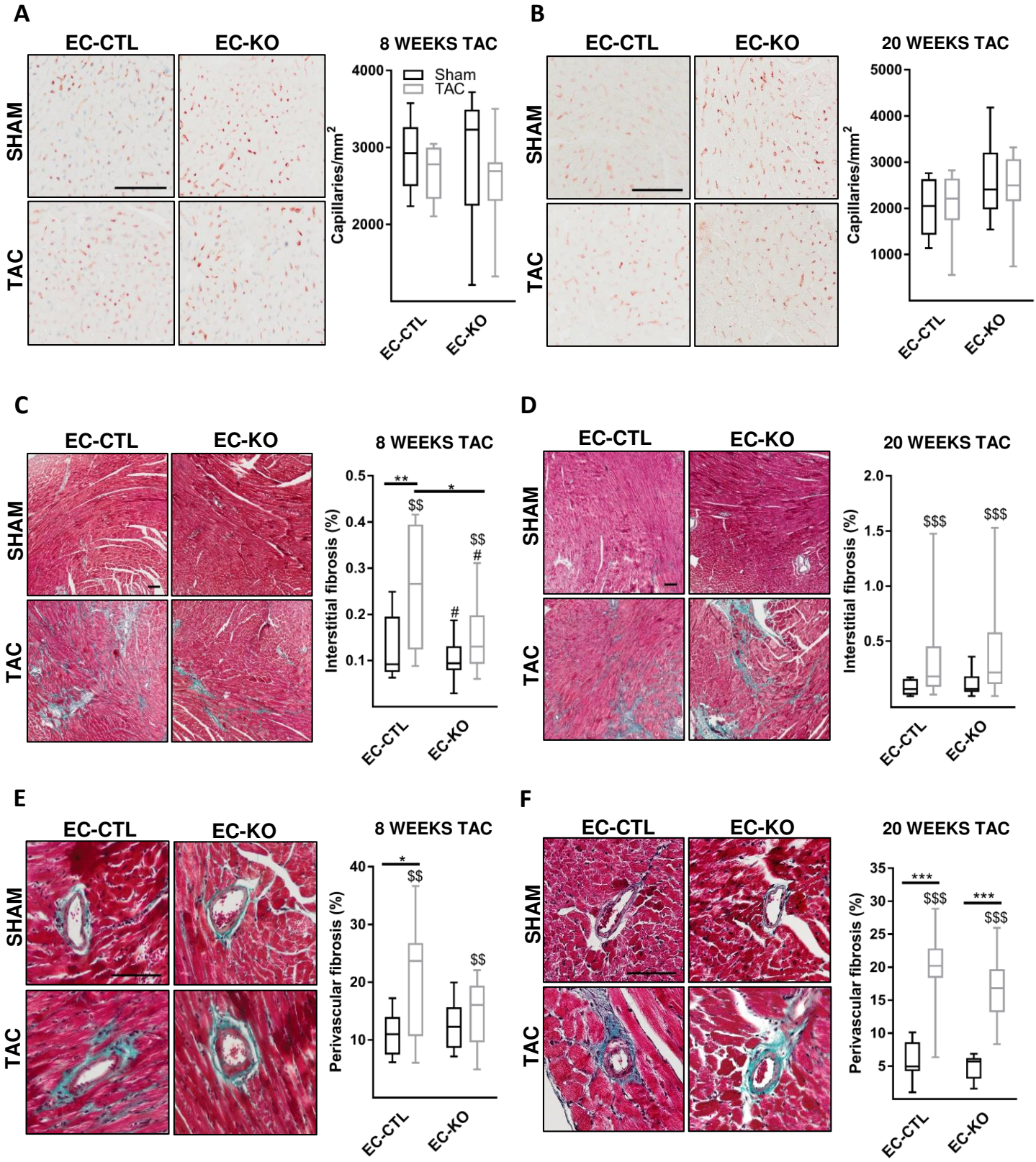

Figure 5

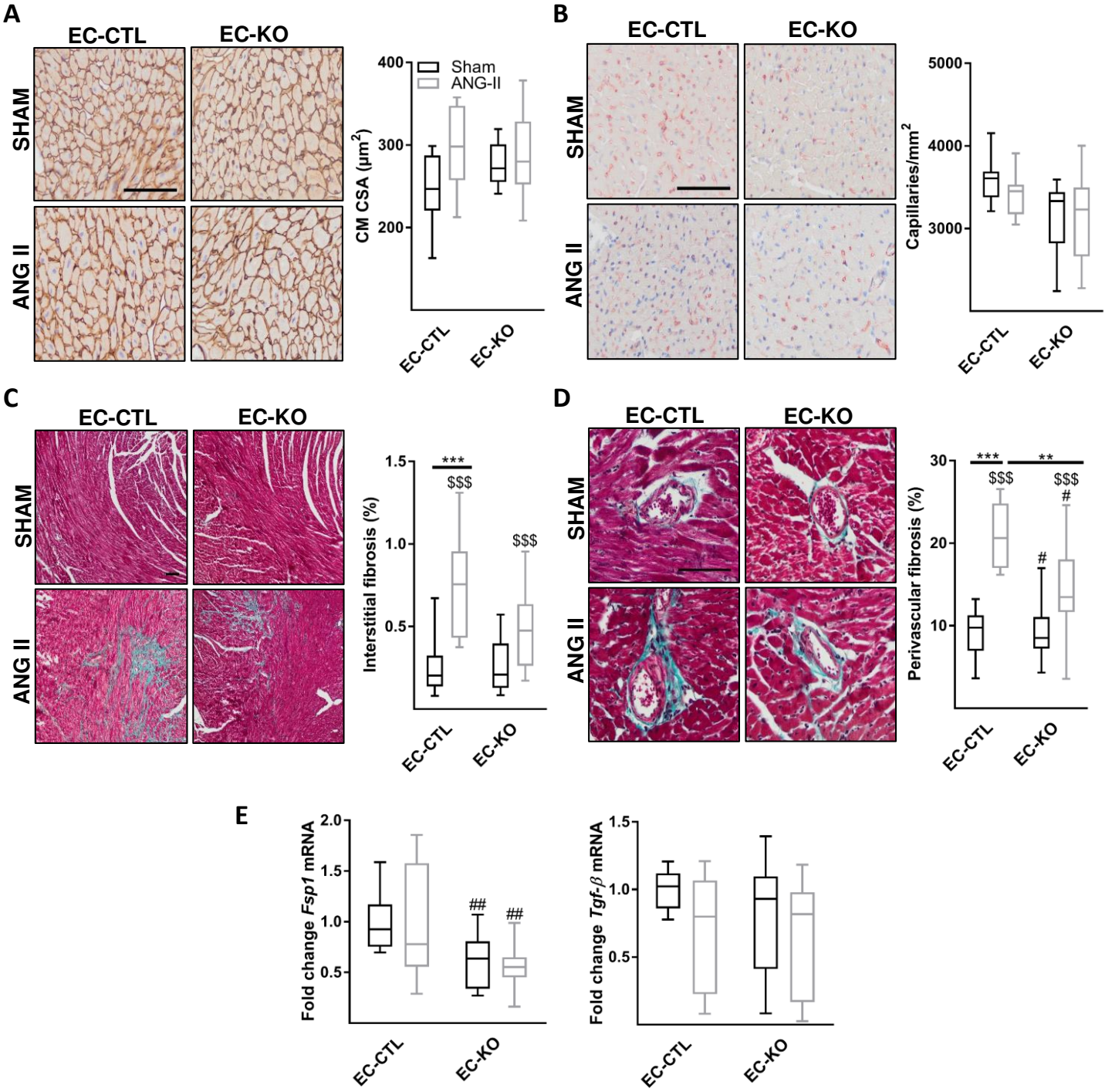

Figure 6